INTERNATIONAL JOURNAL OF CLIMATOLOGY
Int. J. Climatol. 20: 89–104 (2000)

WAVELET ANALYSIS OF THE ASSOCIATION BETWEEN THE SOUTHERN OSCILLATION AND THE INDIAN SUMMER MONSOON

J.R. KULKARNI*
Indian Institute of Tropical Meteorology, Dr. Homi Bhabha Road, Pashan, Pune 411007, India

Received 20 August 1998
Revised 23 March 1999
Accepted 9 May 1999

ABSTRACT

A new aspect of the monsoon–Southern Oscillation (SO) link has been investigated. All India Summer Monsoon Rainfall (AISMR) and Southern Oscillation Index (SOI) data (for August–September–October months) for the period 1871–1998 have been processed for wavelet analysis. Using the Haar wavelet function, the data are decomposed into seven dyadic scales corresponding to periods of 2, 4, 8, 16, 32, 64 and 128 years. The time frequency localization in the wavelet analysis was used to study the temporal variability of modes in AISMR and SOI. The 2 and 8 year modes in both are found to exhibit low frequency modulation. The 4 year mode in both showed large intermittency. The periods of high/low activities of 2, 4 and 8 year modes were associated with a large/low number of deficient AISMR years. The SOI derived from 2, 4 and 8 year modes in the ENSO years, is found to be related to AISMR variability, at 1% level of significance. The 2, 4 and 8 year modes in AISMR and SOI are found to be correlated at a 5% level of significance. There is a large temporal variability in the correlations of these modes. The occurrences of maxima and minima in these correlations followed a sequence, first in the 8 year mode, then in the 4 year mode and in the end, in the 2 year mode. The reasons for de-association between AISMR activity and SOI in the last 8 years of the present decade have been attributed to (i) the negative contributions by 128, 64, 32 and 16 year modes, (ii) the low activity of 4 and 8 year modes and (iii) the weak correlation between AISMR and SOI in 4 and 8 year modes during this period. Copyright © 2000 Royal Meteorological Society.

KEY WORDS: monsoon variability; Southern Oscillation; wavelet analysis; climatic variability

1. INTRODUCTION

The agriculture economy of India with its large growing population is closely linked with the performance of the summer monsoon rainfall. Therefore, the prediction of All India Summer Monsoon Rainfall (AISMR) has been the topic of intense research for the last 125 years. The progress achieved/methods employed in the prediction problem have been reviewed from time to time (see Krishna Kumar *et al.*, 1995 for the latest review). The developments and improvements in the skills in AISMR prediction occurred due to innumerable monsoon variability studies on interannual scale. The interannual variability in AISMR may be attributed to (i) internal dynamics and (ii) boundary forcings. The internal dynamics comprises of flow instabilities, non-linear interactions and tropical–extratropical interactions. The sea surface temperature (SST), sea ice, snow cover and soil moisture form the boundary forcings (Shukla, 1981). The parameters relating to the boundary forcings, such as: (I) SSTs over (a) east equatorial Pacific, (b) Indian Ocean, and (II) Himalayan snow cover, have been in use in various prediction models for a long time (Krishna Kumar *et al.*, 1995).

The strong connection between the variability of AISMR and El Niño–Southern Oscillation (ENSO) is well-recognized (Sikka, 1980; Pant and Parthasarathy, 1981; Rasmusson and Carpenter, 1983; Bhalme and Jadhav, 1984). The lead–lag correlation studies between Southern Oscillation (SO) and monsoon

* Correspondence to: Indian Institute of Tropical Meteorology, Dr. Homi Bhabha Road, Pashan, Pune, 411007, India. Fax: +91 212 393825; e-mail: jrksup@tropmet.ernet.in

CCC 0899–8418/2000/010089–16$17.50

Table I. Contingency table showing the occurrences of normal and deficient (a) AISMR vs. SOI and (b) AISMR vs. SOI(d) less/greater than −0.955 in the 29 ENSO years

	AISMR		Total
	Normal	Deficient	
(a) SOI			
< -0.955	1896, 1902, 1914, 1923, 1925, 1953, 1969, 1991, 1997	1877, 1911, 1941, 1965, 1972, 1982, 1987	16
> -0.955	1880, 1884, 1887, 1891, 1930, 1932, 1939, 1957, 1976	1899, 1905, 1918, 1951	13
Total	18	11	29
(b) SOI(d)			
< -0.955	1896, 1914, 1923, 1953, 1969	1877, 1905, 1911, 1941, 1965, 1972, 1982, 1987	13
> -0.955	1880, 1884, 1887, 1891, 1902, 1925, 1930, 1932, 1939, 1957, 1976, 1991, 1997	1899, 1918, 1951	16
Total	18	11	29

rainfall showed that the correlation coefficients (CC) were highly significant during concurrent and post-monsoon season. The largest CC = 0.67 (for the data derived from the principal component analysis of pressure field by Wright, 1975) was observed for the August–September–October (ASO) season (Bhalme and Jadhav, 1984). A large number of studies relating to east Pacific SSTs showed that these could be predicted a few seasons ahead (Cane *et al*., 1986; Zebiak and Cane, 1987). This eventually generated the interest in the dynamical prediction of AISMR using general circulation models (GCM). In the Tropical Ocean–Global Atmosphere (TOGA) Numerical Experimental Group, priority was given to the simulation of the seasonal monsoon rainfall using GCMs. The results of the experiment were encouraging (WCRP-80, 1995). Palmer *et al*. (1992) demonstrated that a large fraction of the variability of the simulated AISMR was forced by the SST variations over the Pacific. Therefore, ENSO and ENSO-related parameters have been considered important in the empirical and dynamical prediction of AISMR. In spite of the large number of studies, there are some aspects of the monsoon–SO link that have not been understood adequately. Two of them may be stated as follows.

Although there is a strong relationship between ENSO and the monsoons, out of a total of 29 ENSO years, only 11 are associated with deficient monsoon rainfall years (Table I(a)). Monsoon rainfall variability in the last 8 years of the present decade (1991–1998) demonstrates the complexity in the relationship. During this period, the SOI for the ASO (hereafter referred to as SOI) season was negative

Table II. The distribution of AISMR anomalies (cm) and the contributions from the seven modes to SOI anomalies (mb) during the period 1991–1998

Year	AISMR (cm)	Contributions (mb) from the modes								
		2 year	4 year	8 year	16 year	32 year	64 year	128 year	SOI	SOI(d)
1991	−3.69	−0.394	0.218	−0.695	−0.323	−0.112	−0.71	−0.009	−1.387	0.871
1992	−6.64	0.394	0.218	−0.695	−0.323	−0.112	−0.71	−0.009	−0.598	0.083
1993	4.56	0.244	−0.218	−0.695	−0.323	−0.112	−0.71	−0.009	−1.184	−0.669
1994	8.66	−0.244	−0.218	−0.695	−0.323	−0.112	−0.71	−0.009	−1.613	−1.157
1995	−6.14	−0.244	0.206	0.695	−0.323	−0.112	−0.71	−0.009	0.142	0.657
1996	0.16	0.244	0.206	0.695	−0.323	−0.112	−0.71	−0.009	0.631	1.145
1997	2.06	−1.285	−0.206	0.695	−0.323	−0.112	−0.71	−0.009	−1.310	−0.796
1998	5.11	1.285	−0.206	0.695	−0.323	−0.112	−0.71	−0.009	1.259	1.774

Also presented are the values of SOI and SOI(d) (mb) for this period.

(Table II) (in the four years *viz*. 1991, 1993, 1994 and 1997, the SOI anomaly was less than -1.0) and east equatorial Pacific SSTs were having persistent positive anomalies (Climate Diagnostic Bulletin), however, AISMR during this period, was normal. Thus, it appears that the total SOI (i.e. undecomposed into dominant modes) is inadequate for understanding the monsoon–SO link. The studies were carried out to understand the link using the spectral methods. The power spectra of both AISMR and SOI time series showed the characteristics of white noise. The spectral peaks, significant at 95% confidence level (CL), were found in AISMR in the period range 2.3–2.9 and those in SOI in the period range 3.7, 3.9 and 5 years. The coherence spectrum analysis showed that the coherence between them was in the period bands of 2.2–2.5 year, 3.6–3.8 year and 4.8–5.6 year (Bhalme and Jadhav, 1984).

In recent years, the technique of wavelet transform (WT), which provides additional information regarding the localization of frequencies, has been increasingly used for understanding the monsoon–SO link. The technique of WT is described in detail by Torrence and Compo (1998). Hu and Nitta (1996) found that the strong interaction between AISMR and the ENSO cycle occurs through the significant positive correlations on time scales shorter than 24–30 years and the significant negative correlations on time scales longer than 40 years. Wang and Wang (1996) showed that the principal period of the SO had experienced two rapid changes since 1872, one in the early 1910s and the other in the mid-1960s. The dominant period was 3–4 years in the earliest four decades (1911–1960, except the 1920s), and 5 years in the last two decades (1970–1992). It was most energetic during two periods, 1872–1892 and 1970–1992, but powerless during the 1920s, 1930s and 1960s. The powerless period was dominated by quasi-biennial oscillations. Kestine *et al*. (1998) showed that the time frequency spectra of different series describing ENSO had strong multidecadal variations over the past century. They also found the reduced activity of ENSO in the 2–3 year periodicity range during the period 1920–1960, compared with earlier and later periods. Torrence and Webster (1998) and Webster *et al*. (1998) found that the coherence between AISMR and the SO is in the 2–8 year period band. Torrence and Webster (1999) showed that the time series of a 2–7 year variance indicated the intervals of high ENSO/monsoon variance (1875–1920 and 1960–90) and an interval of low variance (1920–1960). The ENSO/monsoon variance also contains a modulation of ENSO/monsoon amplitudes on a 12–20 year time scale. These studies have clearly demonstrated that the monsoon–SO link operates through a 2–8 year frequency band. Therefore, an attempt is made here to address the problems stated in the previous paragraph, *viz*. (i) the monsoon–SO link in the ENSO years, and (ii) an apparent de-association between monsoon and the SO in the past 8 years, through the understanding of the variability of the 2–8 year frequency band, using discrete WT. As the power spectra of both show white noise character, the total power is nearly uniformly distributed over the frequency range *viz*. from the lowest frequency of one wave over the entire period to the highest frequency, i.e. Nyquist frequency. The resolution in the frequencies decreases logarithmically from high frequency to low frequency. With this condition, it is appropriate to consider the frequencies in the selected bands rather than individually. This is achieved exactly in the discrete WT. In addition to these problems, the climatic variability of the dominant modes in AISMR and SO and the interaction between them is also studied.

This paper is divided into five sections. The discrete WT is briefly described in the Section 2, the data used is described in Section 3. The results are discussed in Section 4 and conclusions are given in Section 5.

2. DISCRETE WAVELET TRANSFORM

The discrete WT are those that use discrete wavelet functions. The discretization of the wavelet function is not completely arbitrary since conservation of the amount of information in the signal is required (Daubechies, 1988; Katul and Parlange, 1995). The discretization is achieved using a logarithmic uniform spacing for the scale discretization with increasingly coarser resolution at larger scales (Daubechies 1988, 1992; Mallat, 1989a,b). These basis functions are given by

$$\psi_{[j]}^{(m)}(y) = a_0^{-m/2}\psi\left(\frac{y - jb_0a_0^m}{a_0^m}\right), \tag{1}$$

where ψ is the mother wavelet, m and j are variable scale and position indices, respectively, a_0 is the base of dilation and b_0 is the translation length in units of a_0^m. The simplest and most efficient case for practical computation is the dyadic arrangement resulting in $a_0 = 2$ and $b_0 = 1$ (Mallat, 1989a,b; Chui, 1992; Daubechies, 1992). These discrete WT have the following properties:

(i) They form completely orthonormal basis functions.
(ii) The number of convolutions at each scale is proportional to the width of the wavelet basis at that scale.
(iii) They produce a wavelet spectrum that contains discrete 'blocks' of wavelet power and is useful for signal processing as it gives the most compact representation of the signal. The non-orthogonal transform is useful for time series analysis, where smooth variations in wavelet amplitude are expected.
(iv) The reconstruction of the original series is straightforward (Torrence and Compo, 1998).
(v) They are free from undesired formal relations between the wavelet coefficients that are found in the continuous WT (Yamada and Ohkitani, 1991a,b).
(vi) However, there is one disadvantage in that the total number of scales is limited (Torrence and Compo, 1998).

In the present work, the Haar function is used as the discrete wavelet function. It is given by

$$\psi(x) = \begin{cases} -1 & \text{for } 0 < x < 1/2 \\ +1 & \text{for } 1/2 \le x < 1. \\ 0 & \text{elsewhere} \end{cases} \tag{2}$$

The Haar function value corresponds to a Fourier spectral window, which decays away from a central wavelength at a slower rate than other wavelets, an important consideration where sharp transitions occur (Howell and Mahrt, 1994). If $N = 2^M$ is the number of observations (i.e. N is an integer power of 2), then the scale index m can vary from 1 to M ($M = \log_2(N)$) and the position index at scale m varies from 1 to $N2^{-m}$. It can be seen that an increase in scale results in a reduction of resolution (e.g. at $m = 1$ there are $N/2$ coefficients, at $m = 2$ there are $N/4$ coefficients, at $m = M$ there is only one coefficient). This arrangement requires $(N - 1)$ coefficients for N points. This dyadic arrangement is well-suited for the variability studies since the small scale features are characterized by more wavelet coefficients (Meneveau, 1991a,b; Katul and Parlange, 1995). For computations of wavelet coefficients and reconstruction of a time series $R(t)$, the formulation given by Howell and Mahrt (1994) has been used in this study. The wavelet coefficient $W^m(b)$ at scale m and location b is given by

$$W^m(b) = \frac{1}{2^m}\sum_{j=1}^{2^{m-1}} [R(2^m(b - 1/2) + j) - R(2^m(b - 1))]. \tag{3}$$

The time series of the deviation from the mean at the ith record is reconstructed as

$$R(i) - \bar{R} = \sum_{m=1}^{M} (-1)^l W^m(b), \tag{4}$$

where $b = 1 + \text{int}[(i - 1)/2^m]$, $l = 1 + \text{int}[(i - 1)/2^{m-1}]$ for $i = 1, 2, \ldots, 2^m$, $\bar{R}$ is the mean of the time series $R(t)$. The time series of the different scales, i.e. $R(m, n)$ are constructed from (4) by keeping m constant.

3. DATA

The AISMR data used in the study are taken from Parthasarathy *et al.* (1992) for the period 1871–1991. A dyadic arrangement has been used, which requires the length of the series in the powers of 2. The series

is updated, up to 1998, to have the length of 128 years ($= 2^7$, i.e. $M = 7$). The AISMR series has a mean $\bar{R} = 85.14$ cm and standard deviation $S = 8.28$ cm. The series is normalized with mean $\bar{R}$ and standard deviation S. Interannual variability is classified as *excess\normal\deficient* according to

$$R(i) > (\bar{R} + S) \backslash (\bar{R} - S) < R(i) < (\bar{R} + S) \backslash R(i) < (\bar{R} - S), \tag{5}$$

where $R(i)$ is the AISMR in the ith year. There are 20 excess years and 20 deficient years. Data for the SOI (Tahiti minus Darwin pressure in ASO) have been taken from the Climate Diagnostic Bulletin. The SOI series has a mean of -0.136 mb and a standard deviation of 0.955 mb.

4. RESULTS AND DISCUSSIONS

4.1. Dual spectrum of the AISMR and the SO

The top panels in the Figures 1 and 2 depict the time series of AISMR (cm) and SOI (mb) anomalies. The series and the variation in wavelet coefficients (not shown) are not smooth, so the approach of using discrete WT seems justified. In the discussions to follow, the term 'modes' and 'scales' are used interchangeably. The time series of seven modes are generated using Equation (4) and are presented in the lower panels of Figures 1 and 2. The terms in the time series give the contributions to total anomaly in each year. In the WT, the power spectral density $E(m)$ corresponding to scale m is given by (Katul and Parlange, 1995; Kulkarni *et al.*, 1999)

$$E(m) = \frac{\overline{(W^{(m)}[b])^2}}{2\pi \ln(2)}, \tag{6}$$

where the overbar represents the average over b. Figures 3 and 4 show the wavelet power spectra of the AISMR and SOI obtained using Equation (6). The energies contained in the modes ($m = 1, \ldots, 7$) are expressed in terms of the percentage of the total energy for convenience. These spectra consist of discrete blocks, as described by Torrence and Compo (1999). The significance of the modes is tested by the Monte Carlo method as given in Torrence and Compo (1999). In this method, 500 random series, having the same mean and standard deviation as that of the AISMR and SOI time series, are generated by using the random number generator. These are arranged in increasing order for each scale. The powers in the scale at serial numbers 450 and 475 form the basis for the testing the significance at 10 and 5% levels. The 2 year mode in AISMR and the 4 year mode in SOI are found significant at the 5% level, which is in agreement with Bhalme and Jadhav (1984). It is also seen that, in addition to the 2 year mode, the 4 and 64 year modes are found to be significant at the 10% level in both. These results are in agreement with Torrence and Compo (1999). The existence of the 64 year mode in AISMR was not shown explicitly in the earlier studies, but its presence was detected in the studies related to decada variability of the AISMR (Parthasarathy *et al.*, 1992). Kripalani and Kulkarni (1997) showed that there are 30 year epochs of above and below normal AISMR. In the analysis of AISMR made by Kripalani and Kulkarni (1997), an 11 year running mean of AISMR is carried out which effectively filters out the modes with a period less than 11 years. In the process, the two significant modes of period 2 and 4 years are filtered out and the analysis reveals the remaining significant mode of a 64 year period.

The power spectrum in WT has an additional feature called the *temporal standard deviation of energy*, which is given by

$$\text{S.D.} = \frac{1}{2\pi \ln(2)} [(\overline{W^{(m)}[b]^4}) - (\overline{W^{(m)}[b]^2})^2]^{1/2}. \tag{7}$$

There is no counterpart for this term in the Fourier transform, as for each frequency, the energy is distributed uniformly over the signal. Meneveau (1991a,b) showed that the plot of $E(m) + \text{S.D.}$ gives a compact representation of the energy and its temporal variability at each scale, which is referred to as the *dual spectrum*. However, as shown by Katul and Parlange (1995), a better dimensionless indicator for the temporal energy variance is given by the coefficient of variation of energy, CV(m) defined as

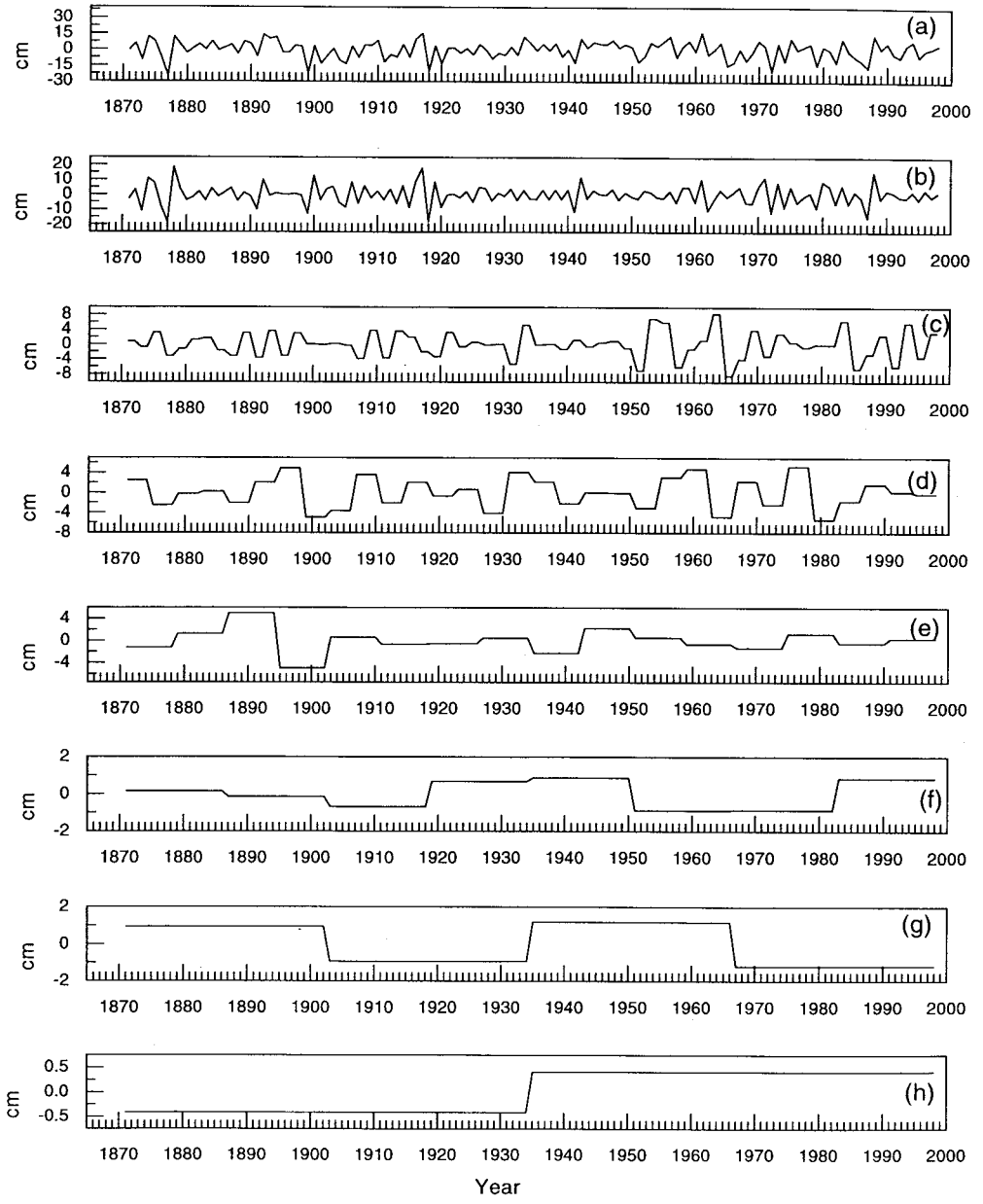

Figure 1. Top panel—(a) AISMR anomaly (cm) for the period 1871–1998. Other panels: time series of (b) 2 year mode, (c) 4 year mode, (d) 8 year mode, (e) 16 year mode, (f) 32 year mode, (g) 64 year mode, (h) 128 year mode in AISMR

$$\mathrm{CV}(m) = \frac{\mathrm{S.D.}(m)}{E(m)}. \tag{8}$$

Figures 5 and 6 show that the plots of CV(m) as a function of scale m for AISMR and SOI, respectively. The Fourier power spectra assume that the power is uniformly distributed with $\mathrm{CV}(m) = 0$ for all m. It may be seen from the figures that $\mathrm{CV}(m) > 1$, that the variation of power is larger than its mean value for the modes 2, 4 and 8 years in AISMR and 2, 4, 8 and 16 years in SOI. The largest variation is found in the 4 year mode indicating the strong intermittent nature of the mode. CV(m) decreases with increasing m, indicating decreasing intermittency in the modes.

4.2. Temporal variability of the dominant modes in AISMR and in SOI

Though the analysis in the previous subsection has shown that the 2 and 4 year modes are significant in both AISMR and SOI, the studies of Torrence and Webster (1998) and Webster *et al.* (1998) have brought out that it is the 2–8 year band which is related to AISMR. Therefore, the 2, 4 and 8 year modes are considered the *dominant* ones in this study. From the total energy point of view, together they contain about 85% of the energy. In order to investigate the temporal variability of these modes, the mean variance contained in the 30 year sliding window have been computed from the time series of the respective modes and are presented in the Figures 7 and 8 for AISMR and SOI, respectively. It is seen

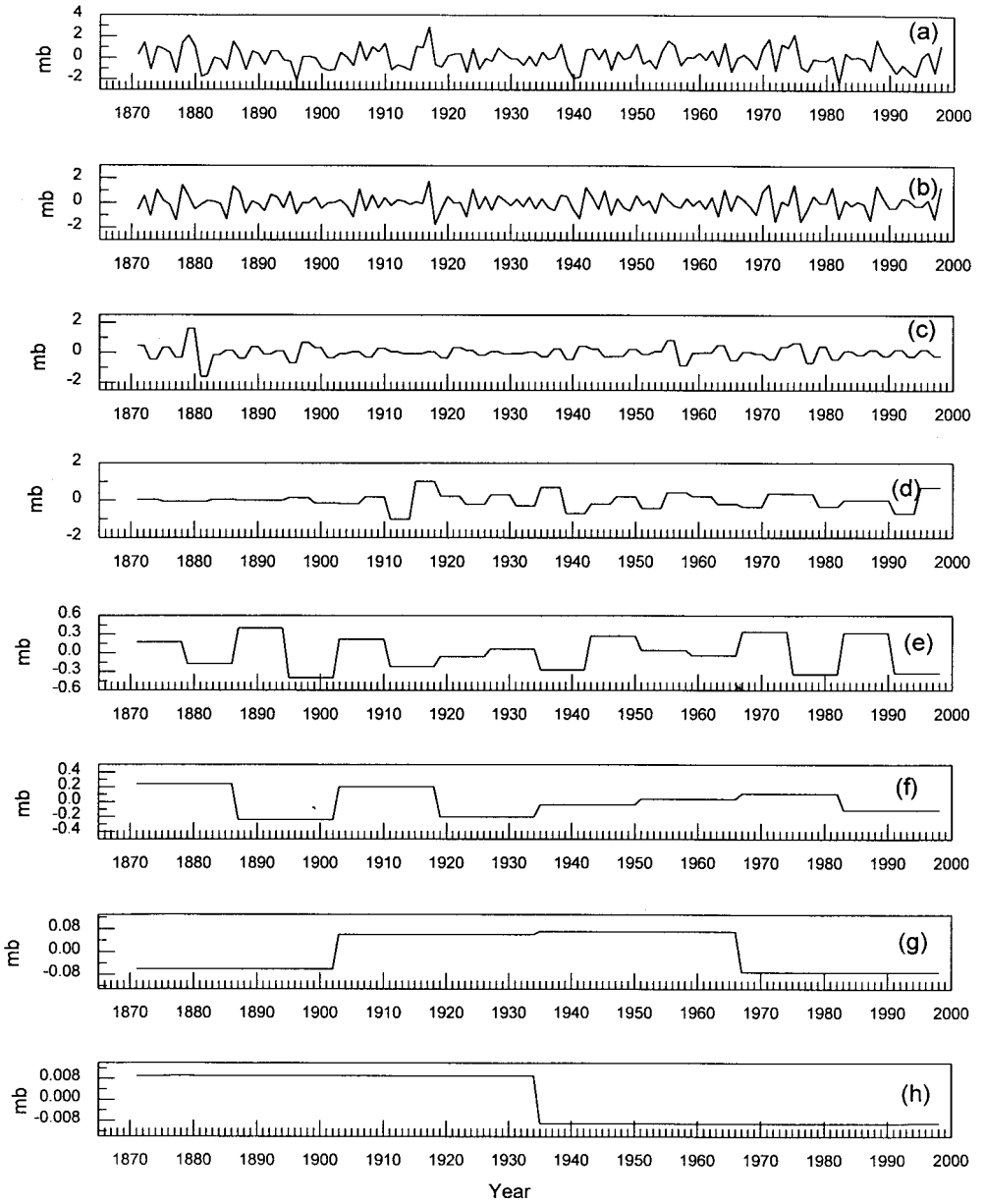

Figure 2. Top panel—(a) SOI (Tahiti minus Darwin) anomaly (mb) for ASO for the period 1871–1998. Other panels: time series of (b) 2 year mode, (c) 4 year mode, (d) 8 year mode, (e) 16 year mode, (f) 32 year mode, (g) 64 year mode, (h) 128 year mode in SOI

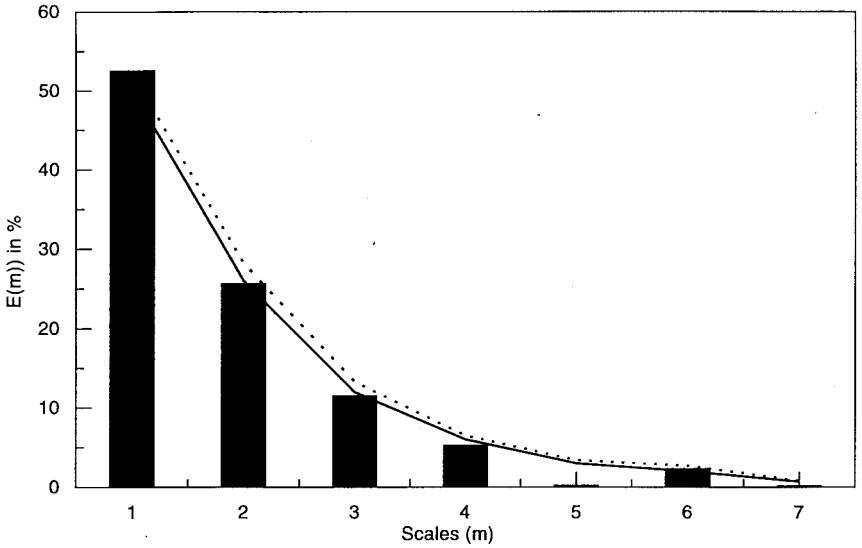

Figure 3. Wavelet spectrum of AISMR for the period 1871–1998. The straight and dotted lines represent 10% and 5% significance levels, respectively

from Figure 7(a) that the activity of the 2 year mode in AISMR undergoes a low frequency modulation, of period 98 and 49 years (significant at the 1% level), reaching peaks in the years 1907 and 1968. The peak in the year 1968 is 1.3 times higher than that in the year 1907. There is a decreasing trend in the activity of the mode in the recent years. The temporal variability of the 2 year mode in SOI (Figure 8(a)) shows a similar feature, however, the peaks around 1910 and 1970 are of nearly equal height. Rasmusson *et al.* (1990), using singular spectrum analysis of equatorial Pacific SSTs and surface zonal winds over Pacific region for the period 1950–1987, showed that the inactive period in the 2 year mode in SOI was during most of the 1950s. The results in the present study are in agreement with Rasmusson *et al.* (1990).

Contrary to the 2 year mode, the 4 year mode presents an intermittent nature. There is a sharp increase in activity of the mode during the 1970s, and a sharp decrease in activity during the 1890s, in both the

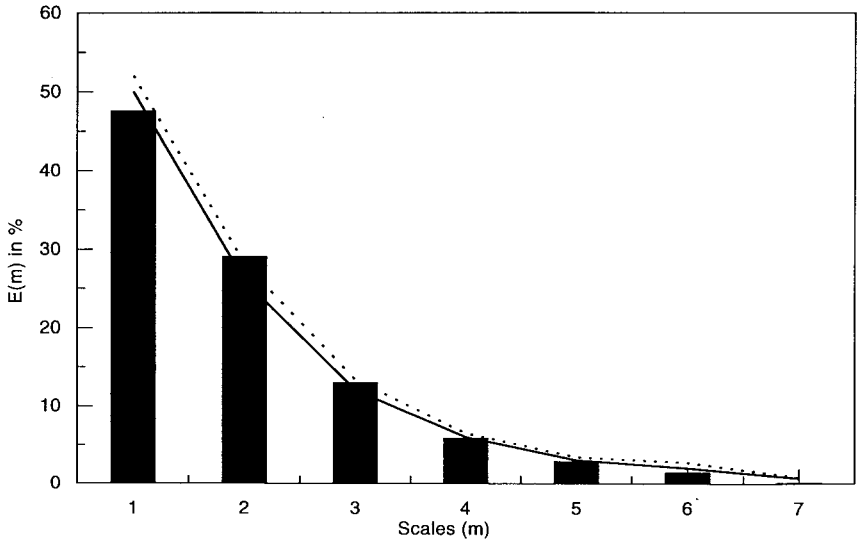

Figure 4. Wavelet spectrum of SOI for the period 1871–1998. The straight and dotted lines represent 10% and 5% significance levels, respectively

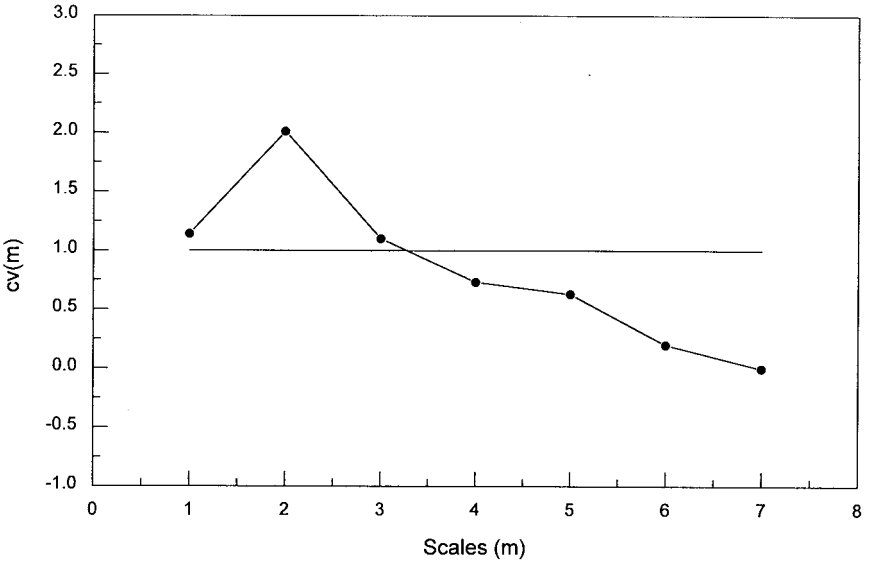

Figure 5. The coefficient of variation, CV(m), in AISMR as a function of scales

AISMR and the SOI (Figures 7(b) and 8(b)). The activity was low during the period 1910–1950. In the recent past years, the activity remained at a constant value. The large coefficient of variation of this mode seen in Figures 5 and 6 can be attributed to the sharp transitions seen in the years of the 1890s and 1970s. The activity of the 8 year mode again showed a low frequency modulation similar to the 2 year mode (Figures 7(c) and 8(c)). The peaks in the mode occurred during 1910s and 1960s, and minimum during 1930s. The similarity in the variability of the modes is striking. The peak around 1910s is higher than that the peak in 1960s. The activity of an 8 year mode is equal to the activity of a 4 year mode during the period 1900–1970 in AISMR. The total higher value of the variance in a 4 year mode compared with that in 8 year mode is due to the high activity of the mode for a very short period during the 1890s and 1970s. Similar to a 2 year mode, this mode also showed a decreasing trend in the recent past years. The low activity of these modes during the 1930s is in agreement with the findings of Wang and Wang (1996) and

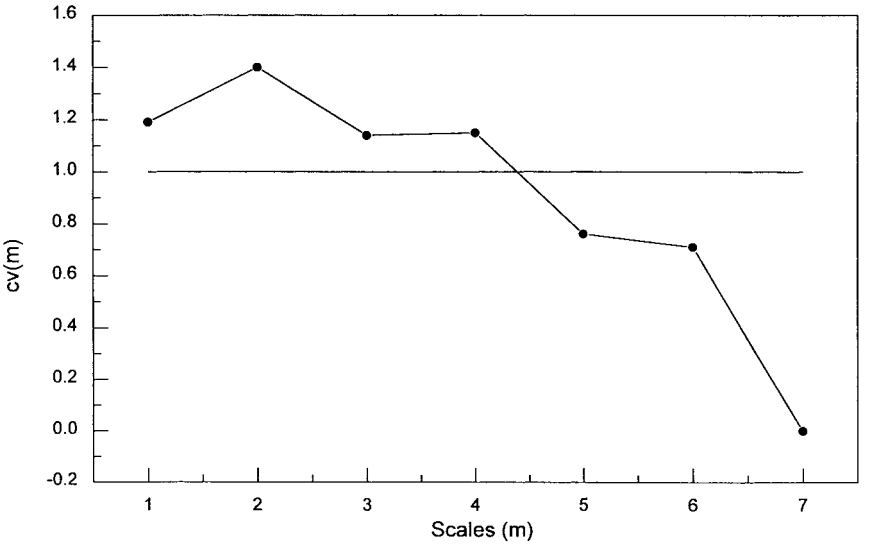

Figure 6. The coefficient of variation, CV(m), in SOI as a function of scales

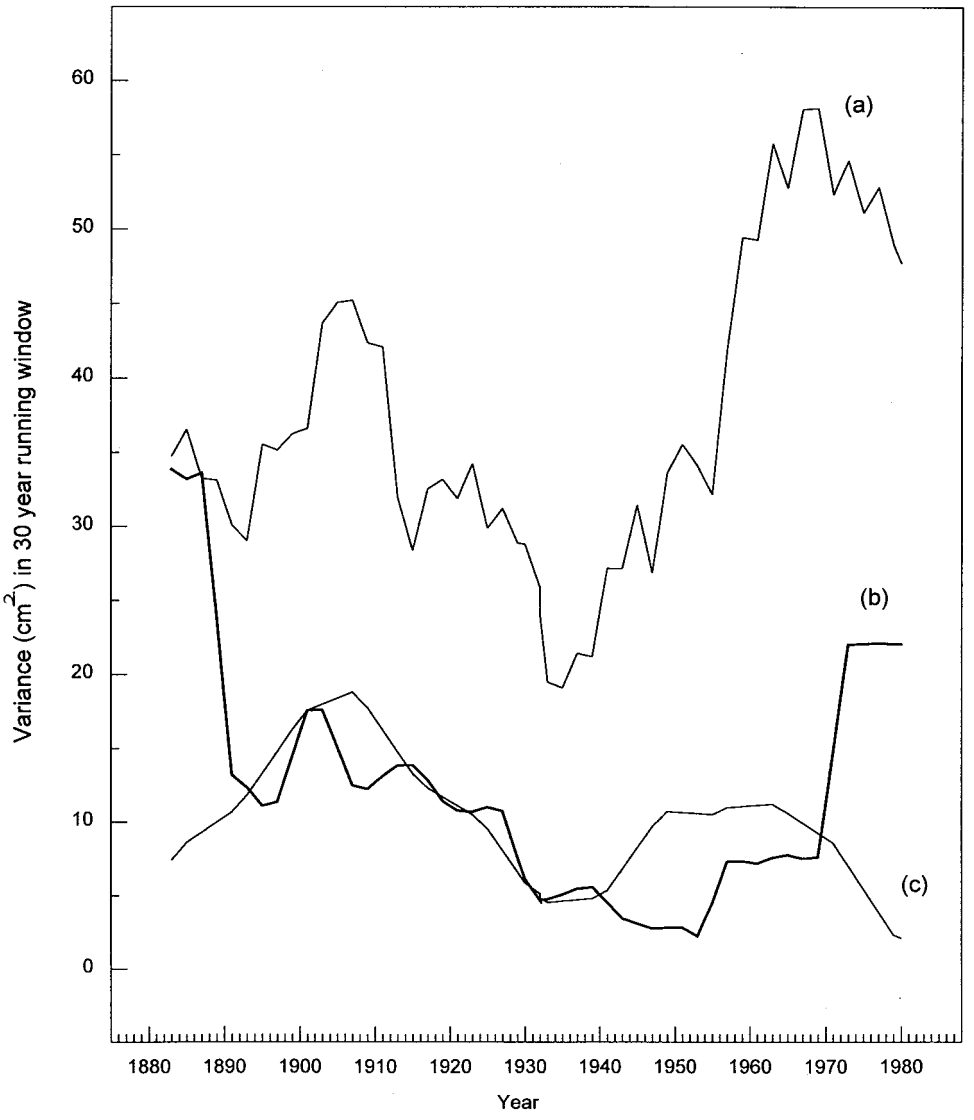

Figure 7. Climatic variability of dominant modes in AISMR; (a) 2 year mode, (b) 4 year mode, (c) 8 year mode

Kestine *et al.* (1998). It is interesting to note that there are two clusters of deficient AISMR years around the 1920s and 1970s, during which the activities of the 2, 4 and 8 year modes are at a peak, and there are a lower number of deficient AISMR years around 1935, during which the activities of the modes are at their lowest level. Further studies are required to understand the sources of these modes in AISMR, and in SOI but it appears that the 2 and 8 year modes may have a different source than that of the 4 year mode.

4.3. Monsoon–SO link

In order to understand the coherency of the individual scales, the sliding correlations between the 2, 4 and 8 year modes in the AISMR and the 2, 4 and 8 year modes in the SOI in a 30 year sliding window have been computed and are presented in Figure 9(a)–(c) along with the 5% significance level. Figure 10(a)–(c) depicts the time series of the product of the terms in the 2, 4 and 8 year modes in the AISMR and SOI. These essentially represent the covariance and also give information regarding phase relationships

among the modes. The positive values indicate that the modes are in-phase while the negative values indicate that the modes are out-of-phase at that location. It is seen that the temporal variability in the correlation of the 2 year mode shows high value of ~ 0.6 during the 1890s, a low and insignificant value of ~ 0.2 during the 1950s, and an increasing trend thereafter. The increasing trend in recent years can be attributed to high covariance during this period as seen from the Figure 10(a). The temporal variability of correlation in the 4 year mode shows bimodal distribution with peaks in the 1900s and 1960s. The correlations have become low and insignificant during the 1980s. This is also in agreement with the high positive coherence during the 1960s and out-of-phase relation of the modes thereafter, as seen from Figure 10(b). The temporal variability in the correlation of the 8 year mode shows high values (~ 0.8) during the 1890s and a minimum during 1935. It also shows low and insignificant activity recently. The low activities during the 1930s and 1960s are due to the out-of-phase relationship of the modes, as seen in Figure 10(c). One interesting feature observed is that the correlation attained the lowest magnitude first around 1935 in the 8 year mode then in the 4 year mode around 1938 and finally in the 2 year mode around 1948.

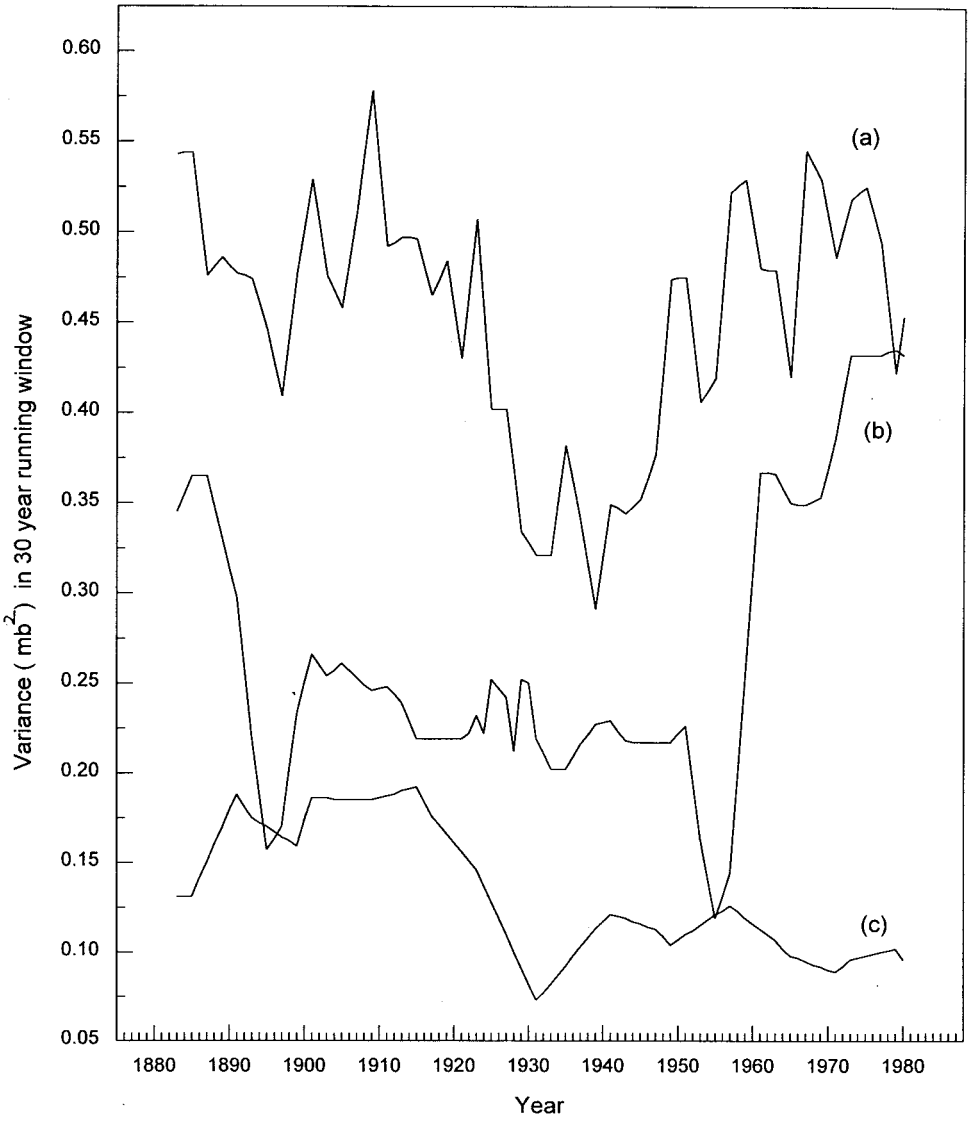

Figure 8. Climatic variability of dominant modes in SOI; (a) 2 year mode, (b) 4 year mode, (c) 8 year mode

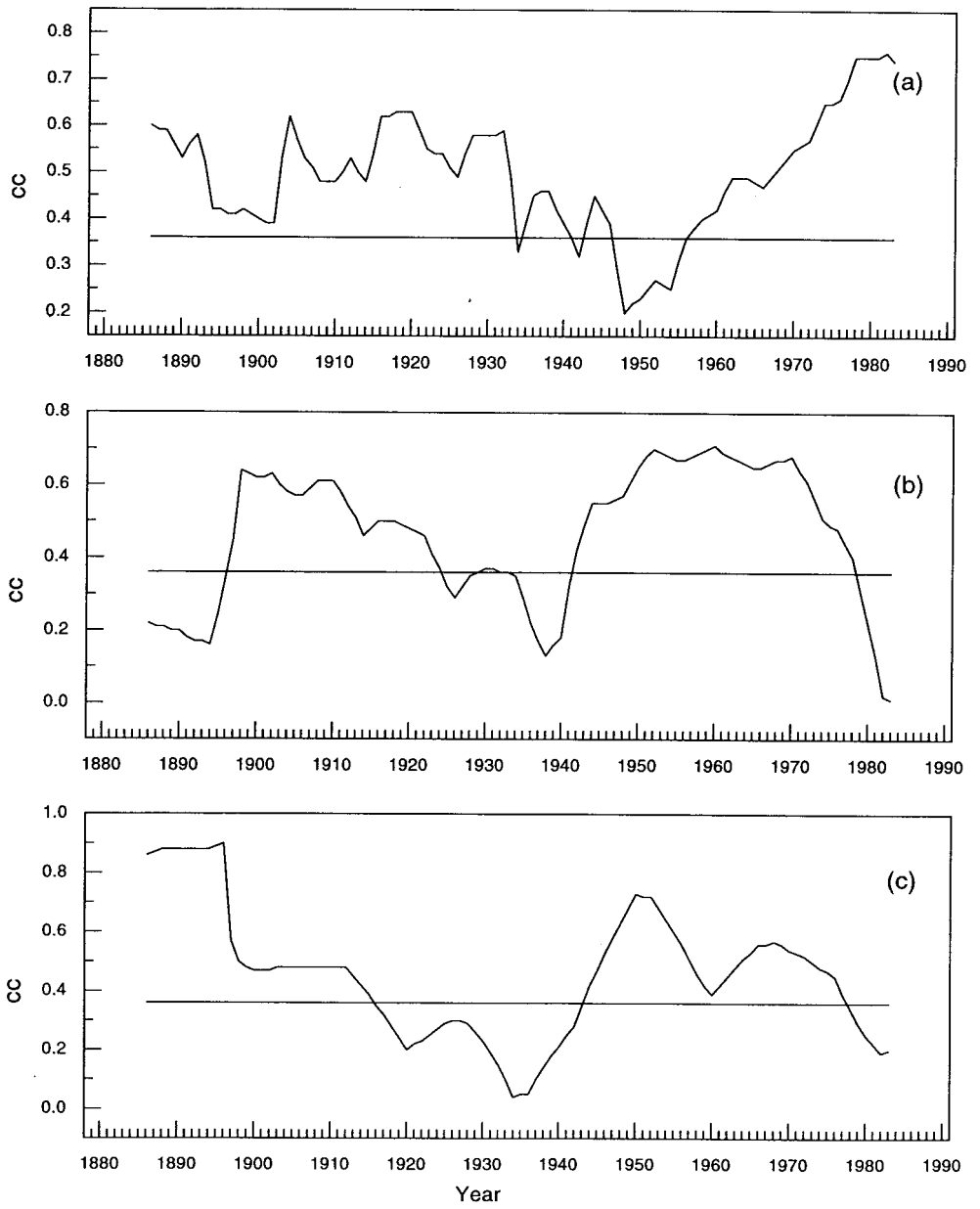

Figure 9. Variation of CC computed between (a) 2 year mode in AISMR and 2 year mode in SOI, (b) 4 year mode in AISMR and 4 year mode in SOI, (c) 8 year mode in AISMR and 8 year mode in SOI. The horizontal line represents the 5% level of significance

Similarly, the second maxima also followed the same sequence, first it is seen in the 8 year mode around the 1950s, followed by the 4 year mode in the 1960s, and then in the 2 year mode in the 1980s.

In order to understand the monsoon–SO link in the ENSO years, the anomalies in AISMR in the 29 ENSO years have been analysed in relation to the total contribution from the 2, 4 and 8 year modes in the SOI, designated as SOI(d). Figure 11(a) and (b) show the scatter plots of AISMR anomaly as a function of (i) SOI anomaly (Figure 11(a)) and (ii) SOI(d) (Figure 11(b)). Though there is an improved relation with SOI(d) (the CC between AISMR anomaly and SOI anomaly was 0.208 and that with SOI(d) was 0.303), it is below the 5% significant level. Therefore, the relation was tested using the chi-square test (with Yates' correction as degrees of freedom is one). Table I(a) and (b) presents the distribution of

AISMR activity (normal and deficient) in the ENSO years as a function of the SOI and SOI(d) anomalies, whether less than or greater than -0.955 mb (minus one standard deviation). It is seen that the number of deficient and normal monsoon years are better related (eight against seven deficient years and 13 against nine normal years) with the SOI(d) anomaly and the relation is significant at the 1% level.

In order to understand apparent disassociation over the last 8 years, the contributions from the seven modes from SOI and SOI(d) in these years have been examined. Table II presents the contributions from the modes and also the AISMR anomalies. It is seen that the contributions from the low frequency modes, *viz*. 16, 32, 64 and 128 years are negative. It is interesting to see that the only period in the total

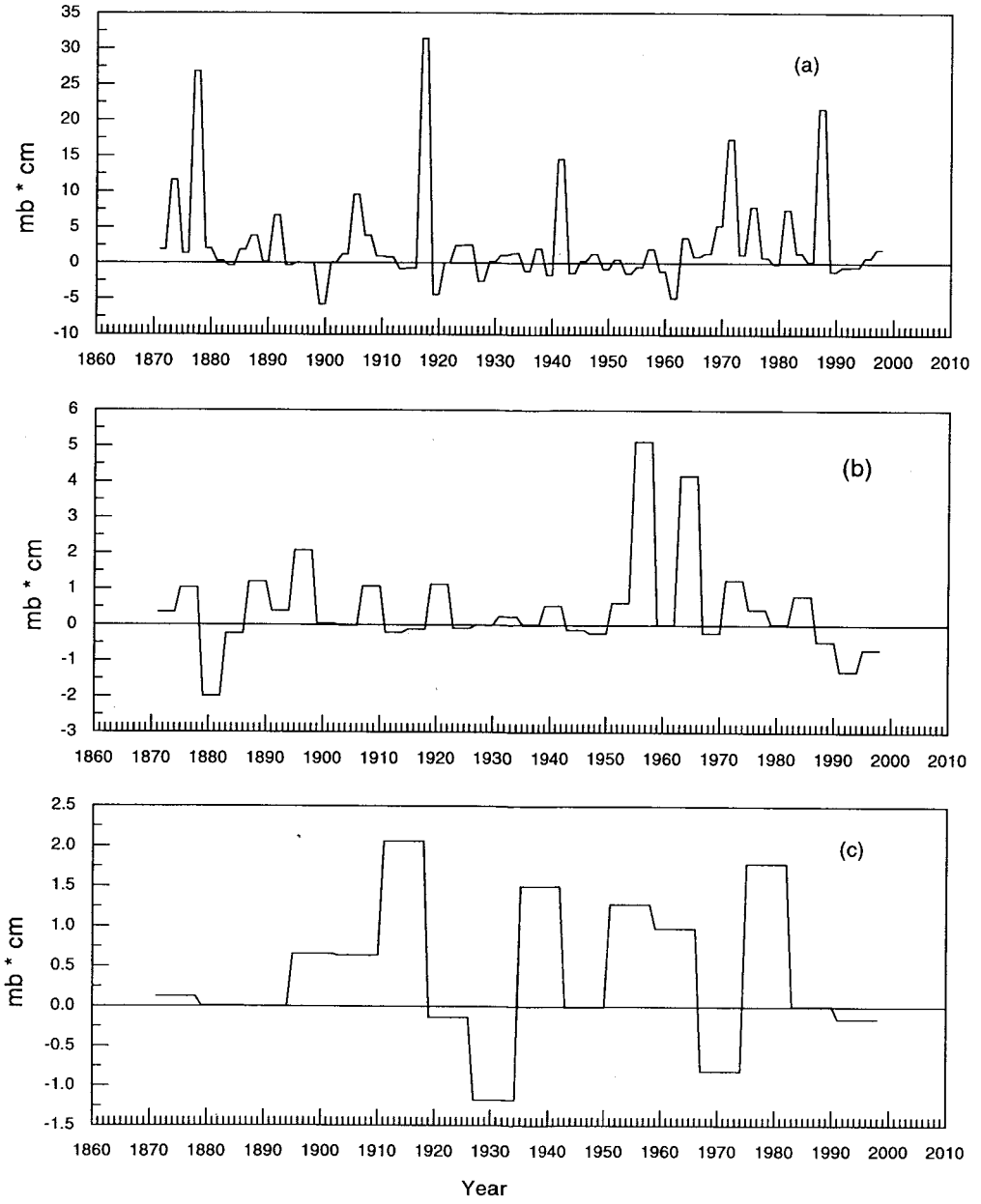

Figure 10. Time series of product of terms in the time series of AISMR and SOI for (a) 2 year mode, (b) 4 year mode, (c) 8 year mode

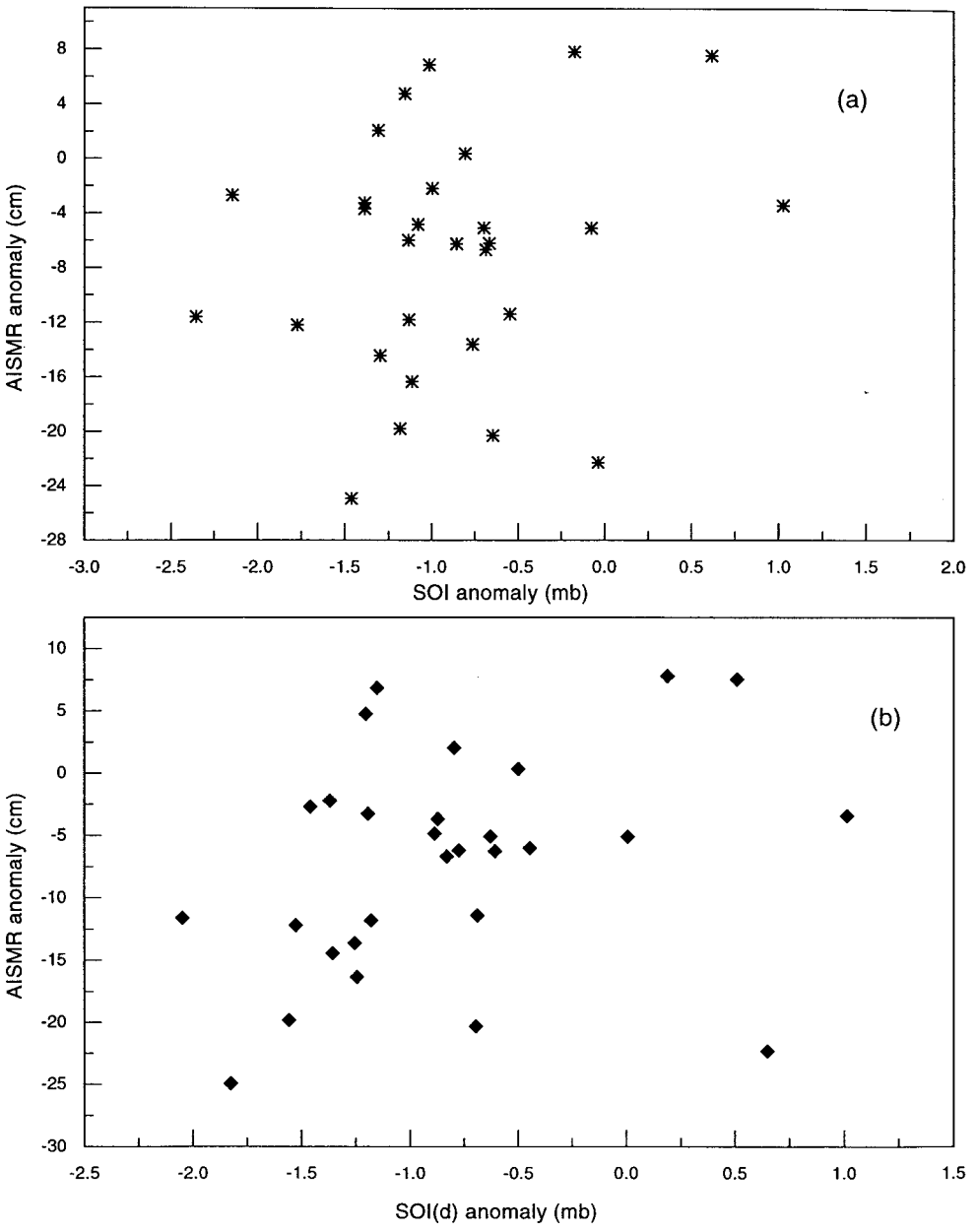

Figure 11. Scatter plots of (a) AISMR anomaly (cm) against SOI anomaly (mb), (b) AISMR anomaly (cm) against SOI(d) anomaly (mb) in the ENSO years

128 year period data, when these modes are in-phase and in the negative side (Figure 2). There are 4 years, *viz*. 1991, 1993, 1994 and 1997, in which the SOI anomaly was less than -1.0 mb. The percentage contributions from the low frequency modes to the total SOI anomaly amounts to 37% in the 1991, 43.5% in 1993, 28.3% in 1994 and 39.2% in 1997. Thus, except in the year 1994, about 40% contribution is from those modes not related to the monsoon activity. Moreover, it can be seen that in the year 1994, the anomaly in SOI(d) is also less than -1.0 mb, but the large part it has been due to the 4 and 8 year modes, which are not significantly related to the AISMR in the present decade. These may be the probable reasons for the normal monsoon activity in the present decade despite the large negative SOI activity.

5. CONCLUSIONS

This study has addressed two important aspects of the monsoon–SO link, *viz*. the monsoon–SO relation in the ENSO years and the disassociation between the monsoon and the SO in the present decade. Though the strong association between the monsoon and the SO was well-established, the occurrence of the majority of normal monsoon years (i.e. 18) in the 29 ENSO years was not clearly understood. This study has revealed that the total contribution from the 2, 4 and 8 year modes from the SOI is related to the AISMR anomalies in the ENSO years at a 1% level of significance.

The temporal variability of the 2 and 8 year modes in the AISMR and SOI shows modulation by a low frequency wave of period of 98 and 49 years at 1% level of significance, respectively. There are sharp transitions in the activities of the 4 year mode in both the AISMR and the SOI, accounting for large intermittency in the power. The periods of high/low activity of the 2, 4 and 8 year modes are found to be associated with a large/low number of deficient AISMR years. The temporal variability in the correlation (based on a 30 year running window) of the 2, 4 and 8 year modes in the AISMR and the SOI show a particular sequence. The maxima and minima in the correlations follow a sequence, first in the 8 year mode, then in the 4 year mode, and then in the 2 year mode. In the present period, the correlations in the 4 and 8 year modes have become insignificant, and that of 2 year mode has started decreasing after the reaching the peak. The activity of the 4 and 8 year modes has remained constant and that of the 2 year mode has shown a decreasing trend. The disassociation between the monsoon and the SO in the last 8 years of the present decade can be attributed to (i) SOI(d) remaining larger than -1 S.D., (ii) reduced activities of the 2, 4 and 8 year modes, and (iii) insignificant correlations in the 4 and 8 year modes. The results in this study will find use in the prediction of AISMR using statistical methods, in which SOI indices are used. As it seems, we are entering the period in which SOI variability will be most likely similar to that observed during the 1930s. The correlations between AISMR and SOI by using the 8 and 4 year modes have already become insignificant and that of the 2 year mode has started decreasing. Thus, it is suggested that the contribution from the 2, 4 and 8 year modes may be considered instead of the original SOI, and probably less weight may be given to SOI as the variability in SOI is heading towards the conditions which prevailed during the 1930s.

ACKNOWLEDGEMENTS

The author is thankful to Dr G.B. Pant, Director I.I.T.M., and Dr V. Satyan, Deputy Director of the Climate and Global Modelling Division of I.I.T.M. for constant encouragement in the study.

REFERENCES

Bhalme, H.N. and Jadhav, S.K. 1984. 'The Southern Oscillation and its relation to the monsoon rainfall', *J. Climatol.*, **4**, 509–520.
Cane, M., Zebiak, S.E. and Dolan, S.C. 1986. 'Experimental forecasts of El Niño', *Nature*, **321**, 827–832.
Chui, C.K. 1992. *An Introduction to Wavelets*, Academic Press, New York.
Daubechies, I. 1988. 'Orthonormal bases of compactly supported wavelets', *Comm. Pure Appl. Math.*, **XLI**, 909–996.
Daubechies, I. 1992. *Ten Lectures on Wavelets*, CBMS-NMF Regional Conference Series.
Howell, J.F. and Mahrt, L. 1994. 'An adaptive decomposition: application to turbulence', in *Wavelet in Geophysics*, Academic Press, New York, pp. 107–128.
Hu, Z.Z. and Nitta, T. 1996. 'Wavelet analysis of summer rainfall over north China and India and SOI using 1891–1992 data', *J. Meteorol. Soc. Jpn.*, **6**, 833–844.
Katul, G.G. and Parlange, M.B. 1995. 'The spatial structure of turbulence at production wavenumbers using orthonormal wavelets', *Bound. Layer Meteorol.*, **75**, 81–108.
Kestine, T.S., Karoly, D.J., Yano, J.I. and Rayner, N.A. 1998. 'Time frequency variability of ENSO and stochastic simulation', *J. Clim.*, **11**, 2258–2272.
Kripalani, R.H. and Kulkarni, A. 1997. 'Climatic impact of El Niño/La Niña on the Indian Monsoon: a new perceptive', *Weather*, **52**, 39–46.
Krishna Kumar, K., Soman, M.K. and Rupkumar, K. 1995. 'Seasonal forecasting of Indian Monsoon Rainfall: a review', *Weather*, **50**, 449–467.
Kulkarni, J.R., Sadani, L.K. and Murty, B.S. 1999. 'Turbulence intermittency in the atmospheric surface layer over Monsoon Trough Region', *Bound. Layer Meteor*, **90**, 217–239.

Mallat, S. 1989a. 'A theory for multiresolution signal decomposition: the wavelet representation', *IEEE Trans. Pattern Anal. Mach. Intell.*, **11**, 674–693.
Mallat, S. 1989b. 'Multiresolution approximations and wavelet orthonormal bases of $L^2(R)$', *Trans. Am. Math. Soc.*, **315**, 69–87.
Meneveau, C. 1991a. 'Analysis of turbulence in the orthonormal wavelet representation', *J. Fluid Mech.*, **232**, 469–520.
Meneveau, C. 1991b. 'Dual spectra and mixed energy cascade of turbulence in the wavelet representation', *Phys. Rev. Letts.*, **11**, 1450–1453.
Palmer, T.N., Brankovic, C., Viterbo, P. and Miller, M.J. 1992. 'Modelling interannual variation of summer monsoon', *J. Climatol.*, **5**, 399–417.
Pant, G.B. and Parthasarathy, B. 1981. 'Some aspects of an association between the Southern Oscillation and Indian summer monsoon', *Arch. Meteorol. Geophys. Bioklim.*, **B29**, 245–252.
Parthasarathy, B., Rupa Kumar, K. and Kothavale, D.R. 1992. 'Indian summer monsoon rainfall indices', *Meteorol. Mag.*, **121**, 174–185.
Rasmusson, E.M. and Carpenter, T.H. 1983. 'The relationship between eastern equatorial Pacific sea surface temperatures and rainfall over India and Sri Lanka', *Mon. Weather Rev.*, **111**, 517–522.
Rasmusson, E.M., Wang, X. and Ropelewski, C.F. 1990. 'The biennial component of ENSO variability', *J. Marine Sys.*, **1**, 71–96.
Shukla, J. 1981. 'Dynamic predictability of monthly means', *J. Atmos. Sci.*, **38**, 2547–2572.
Sikka, D.R. 1980. 'Some aspects of the large-scale fluctuations of summer monsoon rainfall over Indian relation to fluctuations in the planetary and regional scale circulation parameters', *Proc. Indian Acad. Sci. (Earth Planet. Sci.)*, **89**, 179–195.
Torrence, C. and Compo, G.P. 1998. 'A practical guide to wavelet analysis', *Bull. Am. Meteorol. Soc.*, **79**, 61–78.
Torrence, C. and Compo, G.P. 1999. *Interactive Wavelet Plot*, http://paos.colorado.edu/research/wavelets/
Torrence, C. and Webster, P.J. 1998. 'The annual cycle of persistence in the El Niño–Southern Oscillation', *Q. J. R. Meteorol. Soc.*, **124**, 1985–2004.
Torrence, C. and Webster, P.J. 1999. 'Interdecadal changes in the ENSO–Monsoon system', *J. Climatol.*, (in press).
WCRP-80, 1995. 'Simulations and prediction of monsoons. Recent results', *WMO/TD* No. 546, pp. 1–73.
Wang, B. and Wang, Y. 1996. 'Temporal structure of the Southern Oscillation by waveform and wavelet analysis', *J. Clim.*, **9**, 1586–1598.
Webster, P.J., Magana, V.O., Palmer, T.N., Shukla, J., Tomas, R.A., Yanai, M. and Yasunari, T. 1998. 'Monsoons: processes, predictability, and the prospects for prediction', *J. Geophys. Res.*, **103**, 14451–14510.
Wright, P.B. 1975. *An Index of the Southern Oscillation*, Climatic Research Unit, University at East Anglia, Norwich, CRU RP4, UK.
Yamada, M. and Ohkitani, K. 1991a. 'Orthonormal wavelet analysis of turbulence', *Fluid Dyn. Res.*, **8**, 101–115.
Yamada, M. and Ohkitani, K. 1991b. 'An identification of energy cascade in turbulence by orthonormal wavelet analysis', *Prog. Theor. Phys.*, **86**, 799–815.
Zebiak, S.E. and Cane, M.N. 1987. 'A model El Niño–Southern Oscillation', *Mon. Weather Rev.*, **115**, 2262–2278.

